Local human activities overwhelm decreased sediment supply from the Changjiang River
Continued rapid accumulation in the Hangzhou Bay-Qiantang Estuary system

Xie, Dongfeng; Pan, Cunhong; Wu, Xiuguang; Gao, Shu; Wang, Zheng Bing

Important note
To cite this publication, please use the final published version (if applicable).
Please check the document version above.

1   **Local human activities overwhelm decreased sediment from the Changjiang**

2   **River: continued rapid accumulation in the Hangzhou Bay-Qiantang Estuary**

3   Dongfeng Xie[a,*], Cunhong Pan[a], Xiuguang Wu[a], Shu Gao[b], Zhengbing Wang[c,d]

4   [a]Zhejiang Institute of Hydraulics and Estuary, Hangzhou, China.

5   [b]State Key Laboratory for Estuarine and Coastal Research, East China Normal

6   University, Shanghai, China.

7   [c]Faculty of Civil Engineering and Geosciences, Delft University of Technology, The

8   Netherlands.

9   [d]Deltares, P.O. Box 177, 2600 MH Delft, The Netherlands

10   *Corresponding author at: Zhejiang Institute of Hydraulics and Estuary, No.50 East

11   Fengqi Road, Hangzhou, 310020, China.

12   E-mail address: dongfeng.xie@hotmail.com (D. Xie)

13

14   **Abstract:**

15   The aim of this contribution is to investigate the morphological responses of Hangzhou

16   Bay, China, located immediately south of the Changjiang Estuary, to the drastic

17   reduction of the sediment load from the Changjiang River and the large-scale coastal

18   embankment over past decades. The spatial patterns of deposition and erosion, sediment

19   volume changes, and the feedback with hydrodynamics and sediment transport were

20   analyzed, on the basis of historical bathymetric and hydrographic data. The results show

21   that the sedimentation rates in the bay have overall increased rather than decreased over

22   the past decades, despite bed erosion having occurred in the northern bay-mouth. This

23   reveals that the influence of the reduction in the Changjiang River sediment load on the

24 morphological evolution of Hangzhou Bay has to date been insignificant, mainly due to

25 the buffering effect of existing sediment in the outer Changjiang Estuary. The

26 morphological change is mainly related to the implementation process of the coastal

27 embankment. Sediment accumulation induced by progressive seaward coastal

28 embankment has resulted in seaward aggradation from the Qiantang Estuary towards

29 Hangzhou Bay. Analysis of the annually-averaged high and low tidal levels, and

30 durations of rising and falling tides reveals that flood dominance in the inner bay has

31 been increased, due to the coastal embankment and sediment accumulation. The ratio

32 between annually-averaged rising tide and falling tide durations have decreased from

33 0.85 to 0.63. The tidal prism at the interface between the inner and outer bay has

34 decreased by about 25% since 1980s, while the net landward sediment flux has been

35 intensified to a certain extent, which is responsible for the intensifying sedimentation in

36 the inner bay. The local human activities have overcome the decreased sediment from

37 the Changjiang River. Although the coastal embankment will cease in the near future,

38 the morphological response to human activities is expected to continue on for a longer

39 time.

40 **Keywords:** *Morphology; Sediment transport; Tidal asymmetry; Sediment load;*

41 *Hangzhou Bay; Changjiang Estuary.*

42

43 **1. Introduction**

44 Estuaries are defined as semi-enclosed coastal bodies of water which have free

45 connection with the open sea (Fairbridge, 1980). They are unique ecosystems and are

46 often located in densely populated areas (e.g. Kennedy, 1984; Dyer, 1997; Trenhaile,

47 1997; Wang et al., 2015). River discharge, tidal currents, waves and sediment supply

48 are generally the major natural factors controlling the morphological evolution of

49 estuarine environments. On the other hand, morphodynamic development of an estuary

50 is also influenced by human activities such as flood protection, navigation channel

51 dredging, land reclamation, dam construction, or sand extraction. Such human activities

52 frequently cause substantial changes in the configuration of estuaries, their

53 hydrodynamic regime, sediment transport, deposition and erosion patterns (e.g. Van der

54 Wal et al., 2002; Blott et al., 2006; Wang et al., 2002, 2015; Winterwerp and Wang,

55 2013). In many cases the effects of human activities have exceeded changes induced by

56 natural forcing factors. From the coastal management point of view, it is of major

57 importance to understand the processes and mechanisms of morphological responses to

58 human activities and to predict the trends of their future evolution.

59

60 Worldwide, the transport rate of river-borne sediments into most estuaries has

61 apparently decreased in recent decades (Syviski et al., 2005; Milliman and Farnsworth,

62 2011). With the sediment supply reduction, rapid changes have taken place, among

63 them sediment transport adjustments, coastal retreat, slowdown of accumulation, and

64 even onset of erosion (e.g. Milliman, 1997; Syvitski et al., 2005; Yang et al., 2005,

65 2011; Gao and Wang, 2008). The Changjiang River is one of the largest rivers in the

66 world, ranking 3rd in length (6,400 km), 5th in runoff (925 km^3/y) and 4th in sediment

67 load (486 Mt/y) (Eisma, 1998). In the last 30 years, and especially since 2003 when the

68 Three Gorges Dam was constructed and operated, the sediment load at the Datong

69 measuring station located about 640 km upstream of the Changjiang River mouth (the

70 approximate limit of tidal penetration), has decreased drastically from more than 450

71 Mt/y before the1980s to less than 150 Mt/y, in some dry years (e.g. 2006 and 2011)

72　falling below 100 Mt (Fig. 1). As a result, the subaqueous delta of the Changjiang

73　Estuary (CE) has switched from deposition to erosion, and the progradation rates of the

74　fringing tidal flats have slowed down and locally even turned to degradation (Gao and

75　Wang, 2008; Yang et al., 2011; Wang et al., 2015).
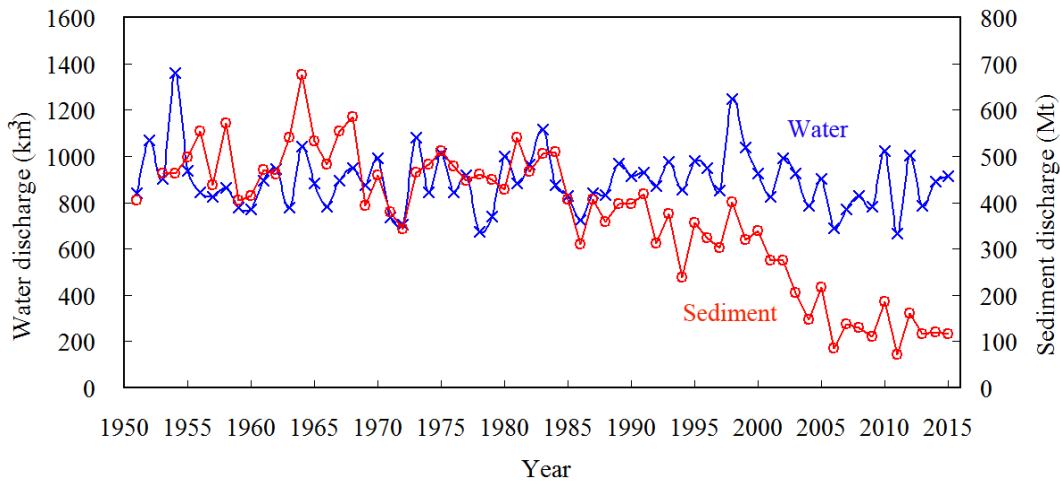
76

77　Fig. 1. Temporal variations of annual water and sediment discharges measured at the

78　Datong gauging station located at the tidal limit 640 km upstream from the Changjiang

79　River mouth (data from the Changjiang River Hydraulic Engineering Committee).

80

81　The Hangzhou Bay, located immediately south of the CE, is one of the largest

82　embayment along the coast of the East China Sea, covering an area of about 4,800 km^2

83　(Fig. 2). Hangzhou Bay is typical funnel-shaped embayment and dominated by tidal

84　currents. The west of Hangzhou Bay, from Ganpu to Zakou, is the Qiantang Estuary

85　(QE), which is controlled by the combination of river discharge and tides (cf. Fig. 2).

86　Hangzhou Bay is an area of extensive material exchange with the Changjiang Estuary,

87　on one hand, and the Qiantang Estuary, on the other (e.g. Chen et al., 1990; Han et al.,

88　2003).
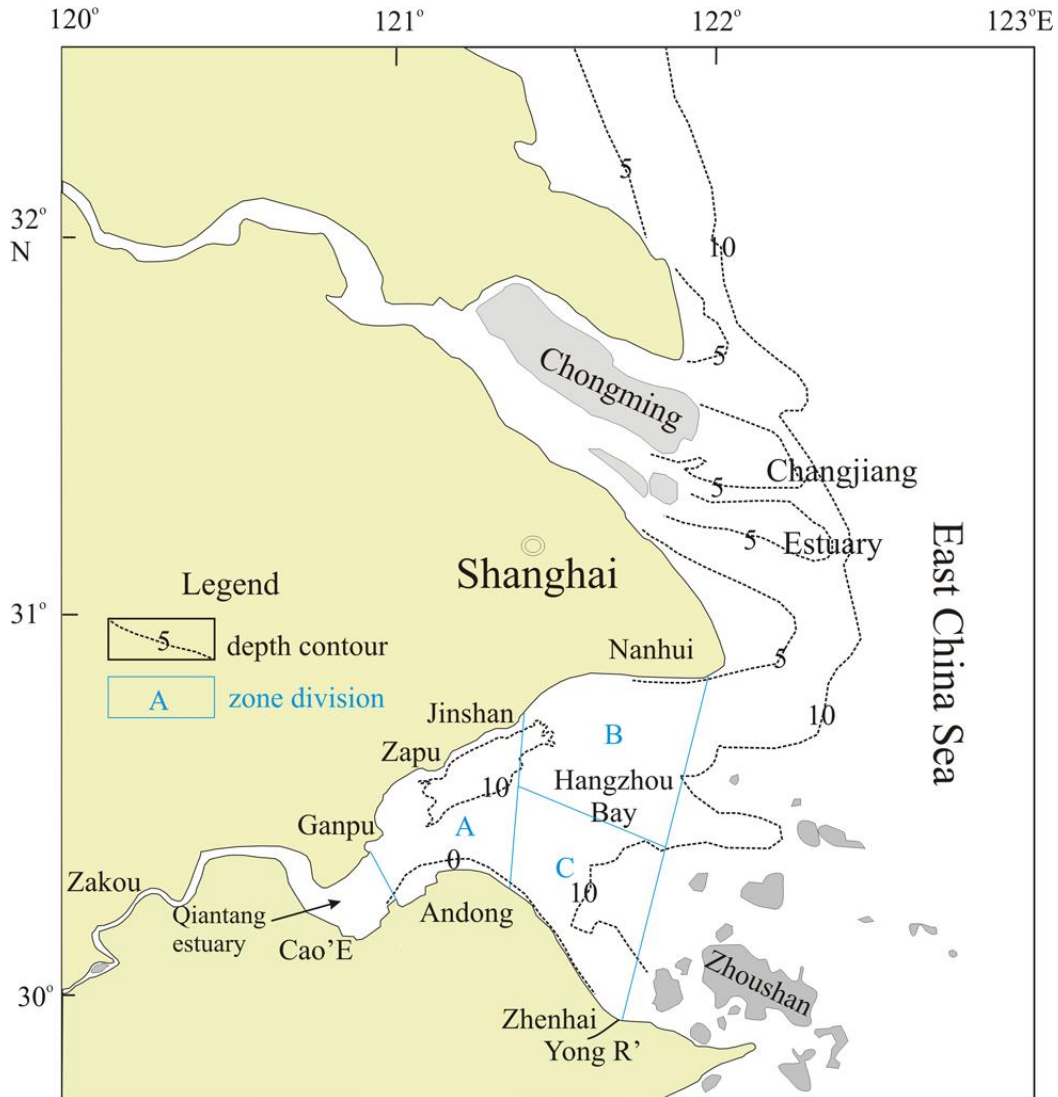
89

Fig. 2. Locations in Hangzhou Bay referred to in the text. The dashed lines depict water

depths. The definitions of the three zones referred to in the statistics of Tables 1 are also

given.

The recent drastic reduction of sediment discharge from the Changjiang River and its

effect on the morphological evolution of Hangzhou Bay have been a matter of great

concern to marine scientists, coastal engineers and the regional management. In recent

years, the northern bay mouth has evolved from an accumulating area to an eroding area,

98   and thought to be related to reduction of sediment discharge from Changjiang River (e.g.

99   Dai et al., 2014). However, little quantitative work has been done on the large-scale

100   morphological response in Hangzhou Bay to such sediment reduction, in particular, on

101   assessing whether the sediment input into Hangzhou Bay has decreased by taking the

102   sediment exchange with the QE into account.

103

104   On the other hand, a large-scale coastal embankment program has been implemented in

105   the QE since the 1960s (Fig. 3), aiming at improving flood protection and navigation (Li

106   and Dai, 1986; Han et al., 2003; Pan et al., 2010). So far, more than 1000 km^2 of tidal

107   flats have been reclaimed, substantially changing the configuration of the estuary. Li

108   and Dai (1986) reported that sedimentation in the QE before the 1980s was mainly

109   caused by the reduction of the tidal prism. They predicted qualitatively that, with the

110   downstream constriction of the QE, accumulation would shift seaward and thereby

111   cause the tidal prism to decrease further. Yu and Cao (2006) documented that

112   sedimentation in the QE from the 1960s to 2000 amounted to about 250×10^6 m^3. The

113   morphological response of the Hangzhou Bay to the embankments is expected to be

114   slower than that of the QE. Recently, Yu et al. (2012) modeled the formation of the

115   large longitudinal sand bar in the QE which elongated 130 km upward of Zapu and

116   occupied the whole QE, using an idealized long-term 2-D model. Their model results

117   showed the sandbar would shift seawards with the increasing convergence of the estuary,

118   and erosion would occur first at the mouth area with the sediment supply decreasing at

119   the sea side. However, their model results were not fully verified due to the lack of

120   detailed information on the temporal evolution of the QE. Although numerous human

121   activities take place concurrently in estuaries, morphologic responses have often been

122 observed to be slow (Wang et al., 2015). To capture the morphological evolution of the

123 Hangzhou Bay, it is therefore necessary to base investigations on more and updated

124 data.
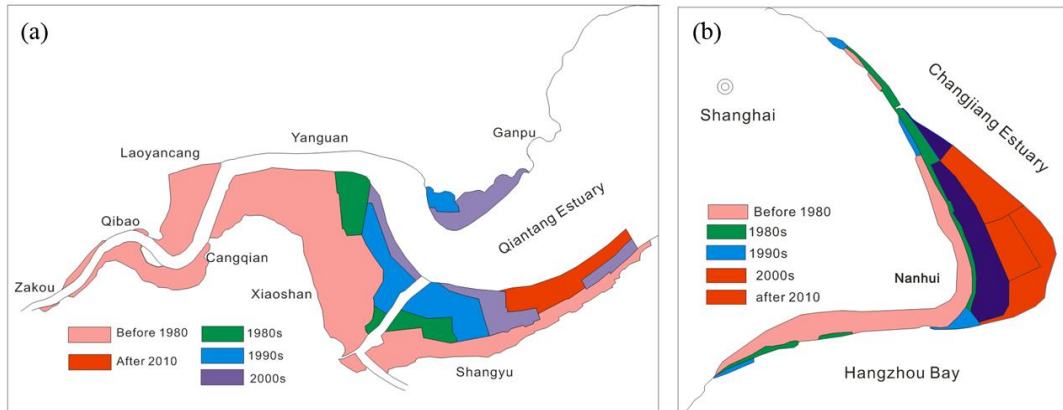
125

126 Fig. 3. Coastal embankment in the Qiantang Estuary (a) and land reclamations in front

127 of the Nanhui flat bordering the Changjiang Estuary (b).

128

129 Short-term changes on more local scales can often be satisfactorily predicted using the

130 so-called 'bottom-up' models, which are based on hydrodynamic models and other

131 process-based computer models, but they have limited capabilities for the prediction of

132 longer-term geomorphological evolution (e.g. Whitehouse, 2002; Townend and

133 Whitehead, 2003). Hence, so-called 'top-down' models, which are based on historical

134 trend analysis, are more frequently used (e.g. Wang et al., 2002; Van der Wal et al.,

135 2002; Lane, 2004; Blott et al., 2006; Yang et al., 2011).

136

137 In this study, several detailed bathymetries of the Hangzhou Bay since 1959, long-term

138 time series of channel volume data of the QE, as well as hydrographic data from

139 representative stations have been compiled. On the basis of these data, deposition-

140   erosion patterns, sedimentation rates for different time intervals, and feedback between

141   hydrodynamics and morphological evolution have been reconstructed. In accordance,

142   the aims of the present study are to clarify whether the sediment supply to the Hangzhou

143   Bay has decreased since the drastic reduction in sediment discharge by the Changjiang

144   River, and to investigate whether any morphological responses are evident in the

145   Hangzhou Bay in response to the large-scale coastal embankments in the region.

146

147   **2. Regional setting**

148   The Hangzhou Bay is normally defined as the reach downstream of Ganpu to the

149   Nanhui-Zhenhai section at the bay mouth (Fig. 2). It is a typical funnel-shaped

150   embayment. The width at the mouth is about 98.5 km and decreases gradually to about

151   20 km some 100 km up-estuary. The total area of Hangzhou Bay amounts to about

152   4,800 km^2. The hydrodynamics and sediment transport are mainly controlled by tidal

153   currents in the bay. Upstream of the Hangzhou Bay, between the cities of Ganpu and

154   Zakou, is the 108 km long QE, which is controlled by the combination of river

155   discharges and tides.

156

157   The Hangzhou Bay can be divided into an outer and an inner part. The outer part from

158   the mouth to Jinshan covers an area of 3,000 km^2 (about 2/3 of the bay) is characterized

159   by a flat seabed with an average water depth of 8~10 m and incorporates numerous

160   scattered islands (Fig. 2). Upstream from Jinshan, the inner Hangzhou Bay covers an

161   area of 1,800 km^2 (about 1/3 of the bay). Between Zapu and the Qibao-Cangqian

162   section, the QE is occupied by a 130 km long, elongated subaqueous sandbar (Chien et

163   al., 1964; Han et al., 2003; Yu et al., 2012). Following the northern shoreline of the

164   middle part of the bay is a large, 60 km long and up to 50 m deep tidal channel, whereas

165   the southern shore is lined by extensive tidal flats. As a whole, the morphology is

166   characterized by sediment accumulation in the south and erosion in the north.

167

168   Runoff and sediment load of the Qiantang River are about 30 km^3/y and 3.40 Mt/y,

169   respectively (Han et al., 2003). Runoff and sediment load of the Changjiang River are

170   925 km^3/y and 486 Mt/y, respectively, being ranked 5th and 4th in the world (Eisma,

171   1998). After the water and sediment enter the sea, one part is dispersed southward into

172   the Hangzhou Bay due to the Changjiang secondary plume, representing the main

173   sediment input to the Hangzhou Bay and the Qiantang Estuary (Su and Wang, 1989;

174   Chen et al., 1990). With the sediment input from Changjiang Estuary, the average

175   accumulation rate in the Hangzhou Bay used to be 1.15 cm/y (Xue, 1995). Despite the

176   fact that the discharge of the Changjiang River has hardly changed over the last few

177   decades, the sediment load has decreased continually since the 1980s, especially from

178   2003 onward when the Three Gorges Dam was constructed and operated (Fig. 1).

179

180   The semidiurnal tide is the main driving force behind the horizontal water flow in the

181   Hangzhou Bay, with the M_2 constituent being the dominant tidal component (ECCHE,

182   1992). The tidal range is 2~4 m at the northern bay mouth, increasing upstream to reach

183   a maximum at Ganpu with 4~6 m. At the southern mouth, the tidal range is only 1~2 m

184   due to the sheltering effect of the Zhoushan archipelago. The deformation of the tidal

185   wave is gradually enhanced upstream due to the progressive constriction of the estuary

186   and the shoaling bathymetry along the large sandbar. This eventually evolves into be the

187   world-famous, Qiantang tidal bore, with the maximum bore height over 3 m and the

188   maximum current velocity up to 5 m/s (Chen et al., 1990; Han et al., 2003; Pan and

189   Huang, 2010). In Hangzhou Bay tidal currents are strong, reaching maximum velocities

190   up to 3 m/s. The northern part is dominated by flood currents, whereas the southern part

191   is dominated by ebb currents. In correspondence, the residual flow and sediment

192   transport directions over one tidal cycle is landward in the north and seaward in the

193   south (Su and Wang, 1989; Xie et al., 2009).

194

195   Sediment in the Hangzhou Bay and the Qiantang Estuary is predominantly composed of

196   well sorted fine-grained non-cohesive silt, with the grain sized between 20 and 40 μm,

197   and transported in suspension (Fig. 4). Suspended sediments in the Hangzhou Bay are

198   vertically well-mixed. Suspended sediment concentration (SSC) in the bay is

199   characterized by three regions of high values separated by two of low values. Average

200   SSCs at the upstream end of the large sandbar, on the southern tidal flat and the

201   northeastern mouth region are 3.4~4.4, 1.2–~3.2 and 1.0~2.6 kg/m^3, respectively,

202   whereas in the southeastern bay and in the northern tidal channels the SSCs are less than

203   1.0 kg/m^3, respectively (Fig. 5). In the QE, the SSC can be more than 10 kg/m^3 at the

204   tidal bore arrival (Chen at al., 1990; Pan and Huang, 2010; Tu and Fan, 2017). Wind

205   generated waves in the bay reach heights of 0.2~0.5 m (ECCHE, 1992).
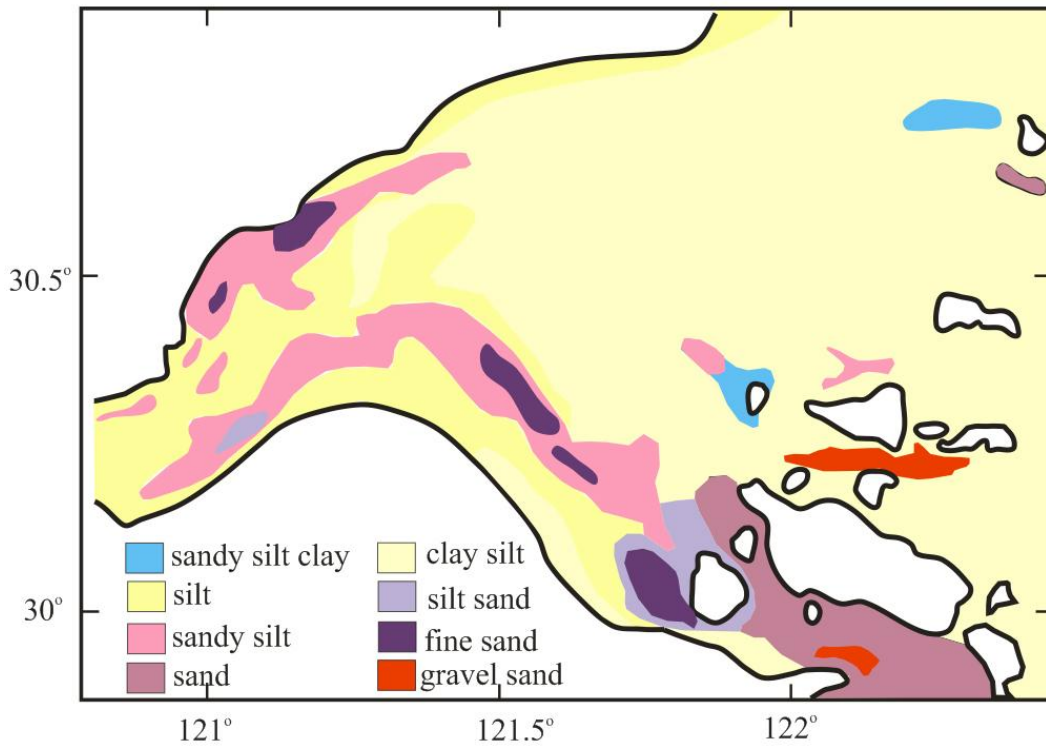
206
207   Fig. 4. Surface sediment grain size in Hangzhou Bay (from Xie et al., 2009).
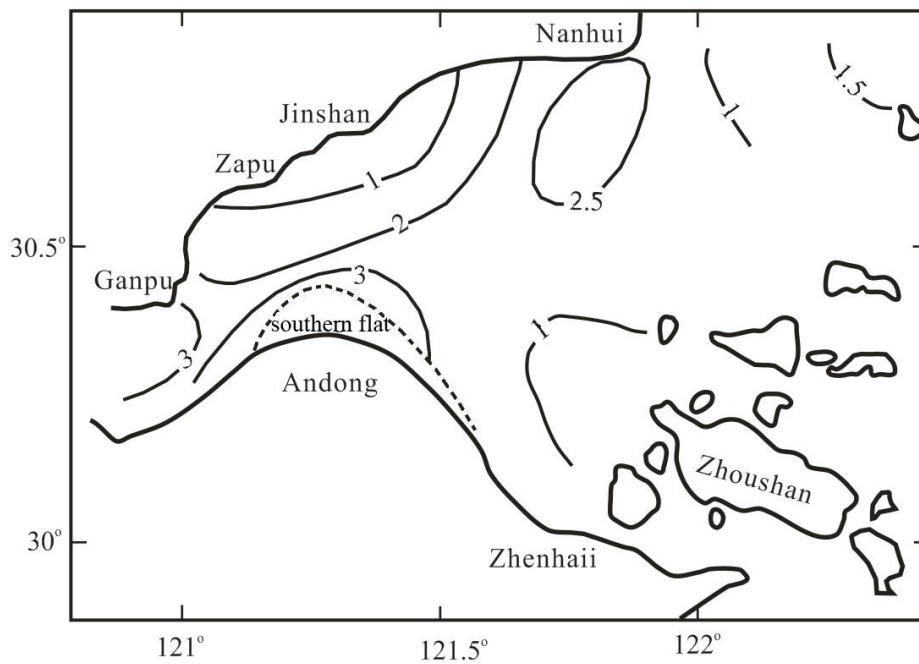
208

209   Fig. 5. Suspended sediment concentration distribution during spring tide in the

210   Hangzhou Bay (modified from Han et al., 2003).

211

3. Materials and methods

3.1 Collection and analysis of bathymetric data

214 Due to the strong hydrodynamics and the easily erodible bed, the bed level of the QE

215 changes drastically on seasonal and inter-annual scales. Maximum vertical bed changes

216 can be up to 5 m in a single year (e.g. Chien et al., 1964; Han et al., 2003). Owing to the

217 importance of the morphology for flood protection, navigation, salt water intrusion, etc.,

218 there are relatively good historical bathymetric time series available for this reach. In

219 this study, the river channel volumes below mean high-tide level in the QE and the

220 inner bay in the month of April of each year since 1980 were collected to quantify the

221 sediment volume changes.

222

223 Available large-scale charts of the Hangzhou Bay mostly only cover the outer

224 Hangzhou Bay or the northern mouth. In this study, detailed and large-scale bathymetric

225 data in the Hangzhou Bay in 1959, 2003, 2010 and 2014, were collected from Zhejiang

226 Surveying Institute of Estuary and Coast (ZSIEC). These data cover the entire bay from

227 the mouth to the Ganpu section. The Odom Hydrotrac echo-sounder was used for the

228 2003, 2010, 2014 data. The vertical error is 0.1 m, and a global positioning system

229 (GPS) by Trimble was used that gave the positioning error within 1 m. The bathymetric

230 tidal corrections used tidal levels recorded at gauging stations within the area of

231 bathymetric data. Bathymetry in 1959 was surveyed by line echo-sounder, with the

232 vertical error less than 1% for water depths greater than 5m. The positioning errors for

233 the 1959 data were 50 m. The accuracy and quality of the bathymetric data depend on

234 the number and density of elevation points along the traverselines used in the

235 bathymetry construction. For the latest three depth measurements, the scales of the

236 maps are 1:50,000 at most area, but 1:10,000 locally, including the tidal flats; for the

237 1959 data, the scale is 1:100,000. These data allowed a detailed analysis of sediment

238 volume changes in the whole bay. As the sediment load from the Changjiang River

239 decreased drastically from 2003 onward, it was possible to determine the bed evolution

240 characteristics of the Hangzhou Bay before and after this date.

241

242 The bed elevation in 1959 was mapped with respect to the theoretically lowest

243 astronomical tidal datum at Wusong, whereas the subsequent surveys were with respect

244 to the Chinese National Vertical Datum of 1985. In a first step the bathymetry maps

245 were digitized using ArcGis10.2 software and then normalized to the theoretically

246 lowest astronomical tidal datum at Wusong. Thereafter, the digitized data were

247 transferred from their original projections onto the Beijing 54 coordinates, the

248 bathymetric data being gridded at 100×100 m resolution using the Surfer software

249 package, making use of the kriging interpolation technique (Burrough and McDonnell,

250 1998), which is appropriate for sparse datasets and has been widely used in previous

251 studies (e.g. Van der Wal and Pye, 2002; Blott, et al., 2006). Subsequently, digital

252 elevation models (DEM) for each digitized bathymetric chart were generated. Spatial

253 deposition and erosion patterns and associated sediment volume changes were

254 calculated by subtraction of the DEMs of different years. The bed level of the reclaimed

255 areas is assumed to be the local average high-tide level, in accordance with the practice

256 of the reclamation procedure. For sediment volume calculations, the bay was divided

257 into three major zones (Fig. 2): the inner Hangzhou Bay upstream of Jinshan (Zone A),

258 the outer, flood-dominated northern Hangzhou Bay where material exchange takes

259 place with the Changjiang Estuary (Zone B), and the outer, ebb-dominated southern

260   Hangzhou Bay (Zone C).The area of each zone approximately corresponds to 1/3 of the

261   Hangzhou Bay. In addition, for each bathymetric chart, the water depths along four

262   transects were extracted for detailed analysis (Fig. 6).

263
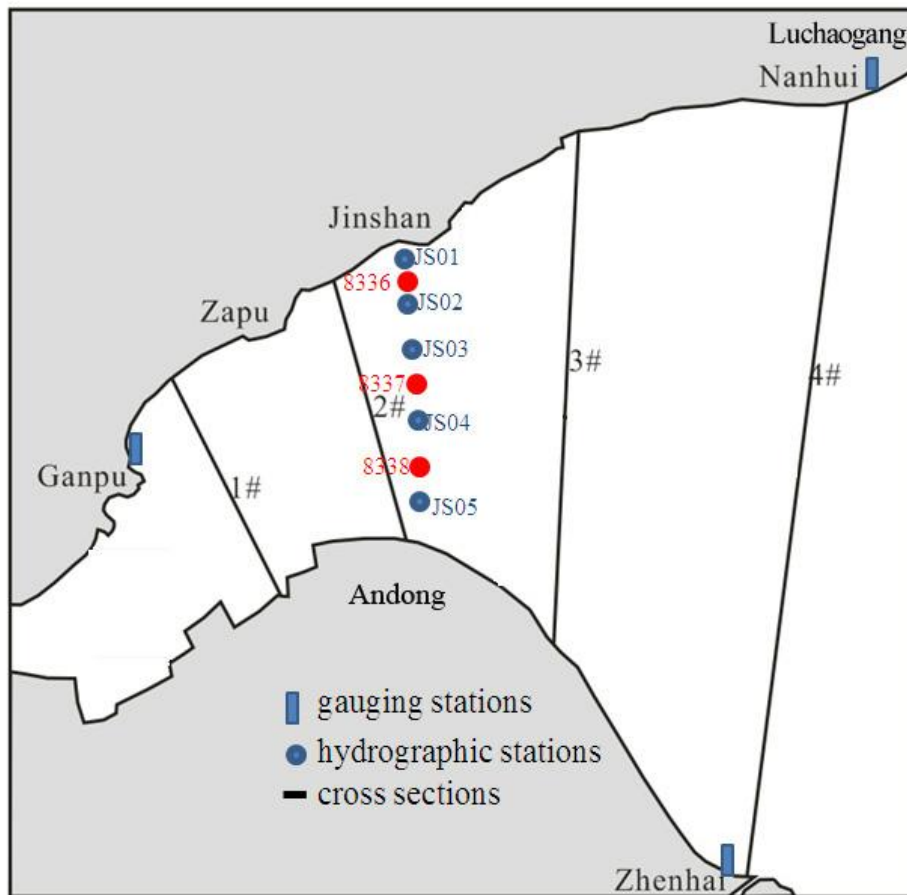
264

265   Fig. 6. The cross-sections illustrated in Fig. 8 and the hydrographic stations of 1983 (red

266   cycles) and 2015 (blue cycles).

267

268   **3.2 Collection and analysis of hydrographic data**

269   Tide levels in the outer Hangzhou Bay and the Changjiang Estuary changed little over

270   the past few decades (Liu et al., 2016), whereas the high-tide level in the inner

271   Hangzhou Bay increased to a certain extent (Han et al., 2003). Hence, time series of

272   tidal elevation at the Ganpu gauging station since 1950s were collected from Zhejiang

273   Hydrographic Office to determine the annually-averaged tidal elevation and duration

274   changes of rising and falling tides and to analyze the non-linear interaction between

275   hydrodynamics and the morphological evolution over the last decades.

276

277   Synchronous hydrographic data along the Jinshan transect, measured in January 1983

278   and January 2015 was collected. The Jinshan transect is the interface between the inner

279   and outer Hangzhou Bay. The cruise in January 1983 was conducted during the

280   Zhejiang Coast Survey, including 4 hydrographic stations restricted to intermediate

281   tides. At all stations, tidal level, water depth, flow velocity, and SSC were recorded. The

282   flow velocities were recorded by Ekman current meters, and SSCs were determined by

283   taking water samples, which were subsequently filtered through pre-weighed paper

284   filters that were weighed after being oven-dried. All water samples, as well as current

285   measurements, were taken at 1 and 5 m below the water surface and at 1 m above the

286   bottom. The cruise in 2015 included 5 hydrographic stations, including spring,

287   intermediate and neap tide. During the cruise in 2015, the measurements at all stations

288   covered at least a full tidal cycle (25 h). During spring tide the measurements were

289   conducted for 36 h. Flow velocities were recorded by means of an acoustic Doppler

290   current profiler (ADCP) and SSCs were measured hourly at the surface, 0.2H, 0.4H,

291   0.6H, 0.8H and the bottom, respectively, using an optical backscatter sensor (OBS),

292   where H is the water depth. Meanwhile, the synchronous tide-level data were collected

293   from several tidal gauging stations including Ganpu, Luchaogang and Zhenhai, etc. (Fig.

294   6).

295

296   Water and sediment fluxes were calculated for various tides of each cruise, with water

297   fluxes being the product of the cross-sectional area and mean velocity, and sediment

298   fluxes being the product of water fluxes and SSCs. The fluxes were calculated per layer

299   and then integrated over the vertical profiles for each tidal cycle by summing the hourly

300   data. For cross-sectional area determinations, the representative distance of each station

301   was defined as the sum of the half-distances between the station and its two neighboring

302   stations. If the station was near the coastline, then the shoreward distance was the

303   distance between the station and the coastline. Because the transects ended at the

304   southern and northern banks, the fluxes represent water and sediment entering or

305   leaving the upper Hangzhou Bay. To examine the tidal influences, the relationship

306   between flood-/ebb-averaged fluxes, i.e. the averaged fluxes over the flood and ebb

307   period, and tidal ranges of Luchaogang station were analyzed. The reason for choosing

308   the Luchaogang station is that it is located outside the bay where the tidal range is not

309   influenced by the morphological changes in the Hangzhou Bay, in contrast to the inner

310   Hangzhou Bay where the tidal range has increased, as will be illustrated later.

311

312   **4. Results**

313   **4.1 Morphological evolution of the Hangzhou Bay**

314   Figure 7 illustrates the rates of morphological change in the Hangzhou Bay over

315   successive periods. From 1959-2003, erosion mainly occurred in the northern channel,

316   while deposition occurred in other parts. This pattern is consistent with the earlier

317   reported historical evolution of the Hangzhou Bay that was characterized by "erosion in

318   the north and deposition in the south" (Cao et al., 1985; Han et al., 2003). These

319 changes were related to large-scale sediment transport induced by the propagation of the

320 tidal wave under the influence of the Coriolis force (ECCHE, 1992). Sediment

321 accumulation during this period was 5.2×10^9 m^3 (Table 1). The sedimentation
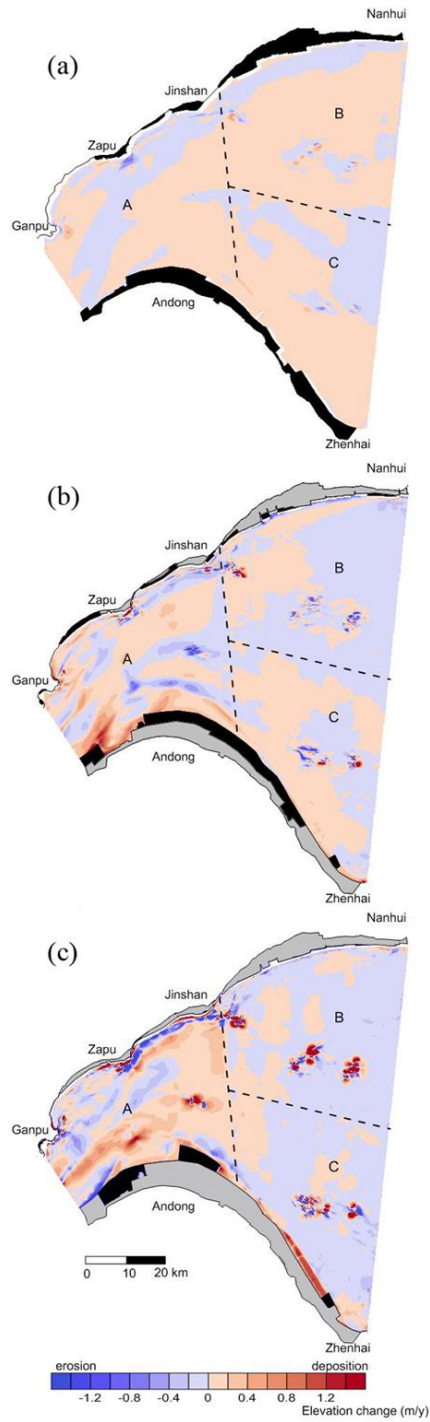
322

323 Fig. 7. Rates of morphological change in Hangzhou Bay over successive periods: (a)

324 1959~2003; (b) 2003~2010; and (c) 2010~2014. The black areas denote land

325 reclamation and the shading areas denote the original shoreline and the latest

326 reclamation.

327 accumulations in the periods 2003~2010 and 2010~2014 were 1.1×10^9 and 0.6×10^9 m^3,

328 respectively. Correspondingly, the accumulation rates in the three periods were 2.4, 3.3

329 and 3.0 cm/y, which indicate a generally increasing accumulation trend. Xue (1995)

330 studied volume changes in the Hangzhou Bay using charts of 1887, 1937 and 1987. His

331 results show that the deposition rates in the Hangzhou Bay were 0.8 and 1.5 cm/y in the

332 former and latter 50 years, respectively and the average was 1.15 cm/y for the 100 year

333 period. This suggests that the sedimentation rates in the Hangzhou Bay increased

334 gradually from 1887 to 2014.

335

336 All three zones (cf. Fig. 2) showed accumulation in the period 1959~2003. In Zone A

337 (the inner bay) the rate was 2.4 cm/y, and those in zones B and C (the northern and

338 southern parts of the outer bay), were 1.0 and 3.9 cm/y, respectively. In the periods

339 2003~2010 and 2010~2014, the accumulation rates in Zone A were 9.0 and 13.4 cm/y,

340 revealing a 2.5- and 4.5-fold increase compared to the period 1959~2003. The sediment

341 deposited in the subaqueous area of Zone A since 1959 amounted to 2.36×10^9 m^3,

342 indicating an average bed-level change of about 1.47 m. Zone B switched from

343 accumulation to erosion in the latter two periods, the rates being -4.0 and -1.9 cm/y,

344 respectively. Zone C maintained the accumulating trend from 2003 to 2010, but also

345 switched to erosion from 2010 to 2014, the rates being 5.8 and -1.3 cm/y, respectively.

346

347 **4.2 Changes in cross-sections**

348 Cross-sections of the inner and outer parts of the bay illustrate the bed-level changes in

349 greater details (Fig. 8). Along cross-sections of the inner bay (1# and 2#), the overall

350 sedimentation can be observed, with the averaged elevations of the sea bed increasing

351 by around 1.5 m. Notable strong sedimentation occurred at the southern bank. The

352 shoreline in the south advanced by about 6 km and 12 km in cross-section 1 and 2#,

353 respectively, since 1959 due to embankment by dyke buildings. The southern flat above

354 mean sea level (MSL) advanced correspondingly and the slope above MSL steepened

355 gradually. Strong sedimentation occurred at the front of the flat (sub-tidal area below

356 MSL) from 1959 to 2003, with the maximum sedimentation of about 5m, indicating a

357 sedimentation rate of about 11 cm/y. The average slopes of the front area of 1 and 2#

358 increased from 1.2‰ to 2.5‰ and from 0.9‰ to 1.7‰, respectively. The steeper slope

359 was more or less maintained during 2003 and 2014. This is probably because the

360 development of the front area of the southern flat is constrained by the main channel of

361 the Hangzhou Bay (Chen et al., 1989). The erosion in the front of 2# between 2003 and

362 2010 is probably caused by the embankment enhancing the current in the adjacent area.

363

364 Along cross-section 3#, the southern channel-shoal system that existed in 1959

365 disappeared and the bed became smooth. From 1959~2003, the northern part accreted

366 vertically by about 1 m, and the southern shoreline advanced by about 5 km and

367 accreted by about 3.5 m, with the sedimentation rate being about 8 cm/y. After 2003 the

368 bed showed slight accumulation with a maximum of about 0.7 m.

369
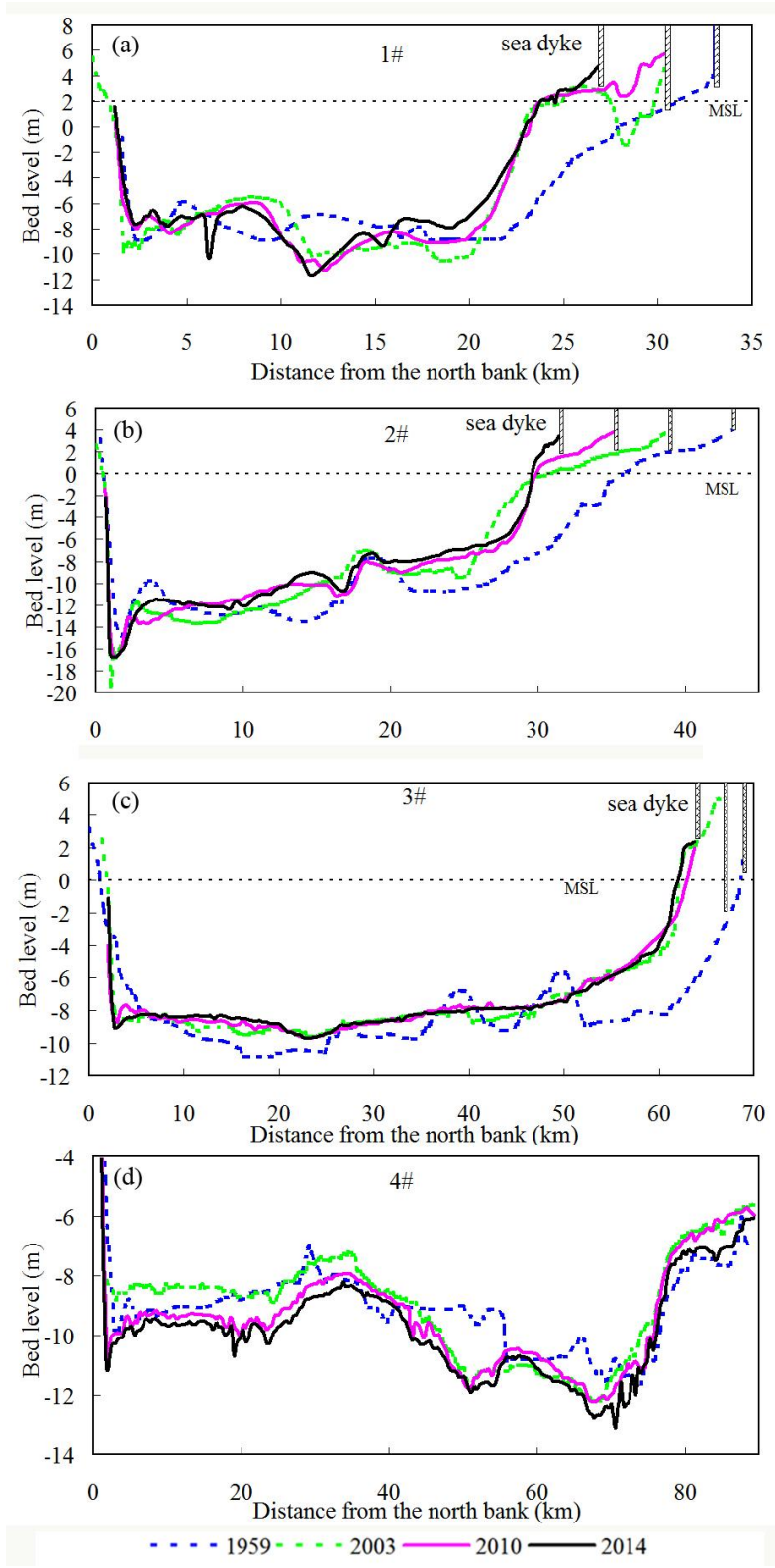
370

371   Fig. 8. Bed level changes along the cross-sections depicted in Fig. 6.

372　Cross-section 4#, located at the bay mouth, showed accumulation in the northern and

373　southern parts, but erosion in the central part in the period from 1959~2003, on average

374　amounting to about 1 m. From 2003-2010 the most remarkable change was the up to 1

375　m erosion at the northern mouth. From 2010-2014 the whole section along the mouth

376　eroded about 0.4 m.

377

378　**4.3 Morphological evolution of the Hangzhou Bay-Qiantang Estuary system**

379　There are strong water and sediment exchanges between the Hangzhou Bay and the QE

380　(e.g. Chen et al., 1990; Han et al., 2003). In the last decades, the bed change in the QE

381　was characterized by continuous accumulation, which was mainly caused by artificial

382　coastal embankments since the 1960s, which resulted in constriction of the estuary (Li

383　and Dai, 1986; Han et al., 2003; Pan et al., 2010).

384

385　Figure 9 illustrates time series of channel volumes below the mean high-tide level of the

386　QE and the inner bay since 1980. Channel volume decreases indicate accumulation.

387　Before 1993, the volume in the QE was basically stable, fluctuating around an average

388　of about $4.1 \times 10^{9} \, \text{m}^{3}$. From 1993~2005, the volume continuously decreased with the rate

389　of $71 \times 10^{6} \, \text{m}^{3}/\text{y}$, and the accumulate rate being 10.2 cm/y. The fluctuation of volumes

390　between neighboring years should be attributed to the variation of the water discharge

391　from Qiantang River. The bed level change in the QE is sensitive to the river discharge

392　because the fine sediment in the estuary can be easily resuspended. The seabed of the

393　QE tends to be eroded during high flow season or years, and deposited during low flow

394　season or years (Chien et al., 1964; Han et al., 2003; Yu et al., 2012). After 2006, a new

395　relatively stable volume reached with an average channel volume of $3.0 \times 10^{9} \, \text{m}^{3}$. For the

396 inner bay, the bathymetric data was deficient before 1986. Since 1986, the volume

397 decreased stepwise in two stages. From 1986~2005, the average volume change was

398 about 74×10^6 m^3/y, whereas since 2006 it doubled to about 150×10^6 m^3/y (Fig. 9).

399 Correspondingly, the accumulation rates were 4.4 cm/y and 9.0 cm/y, respectively. It is

400 interesting to note that the difference between the average volume changes before and

401 after 2006 (76×10^6 m^3) was almost identical to that of the QE in the period from

402 1993~2005. This suggests that, when the morphological evolution of the QE was

403 relatively stable, the location of sediment deposition moved seaward to the inner

404 Hangzhou Bay. The total accumulation rate of the two areas together remained more or

405 less constant.
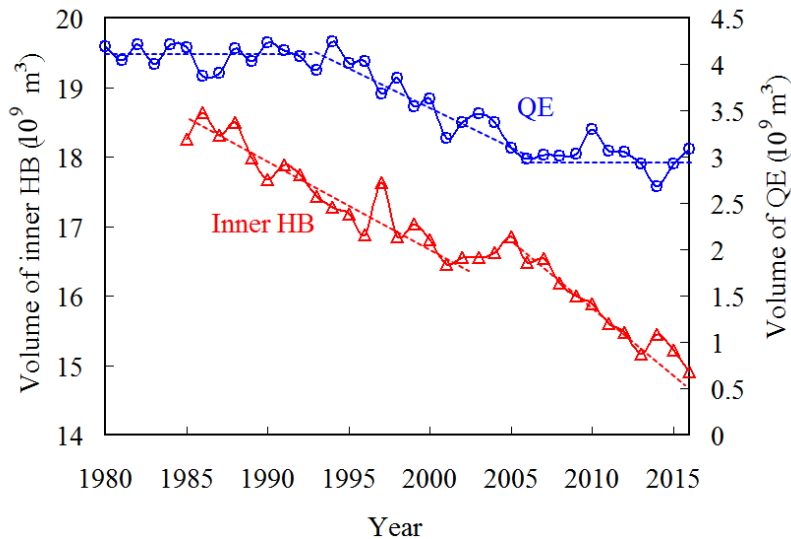
406

407 Fig. 9. Temporal changes in channel volumes below mean high-tide level in the

408 Qiantang Estuary and the inner Hangzhou Bay (zone A in Fig.2).

409

410 Table 2 lists the channel volume changes of the QE and the Hangzhou Bay in the same

411 periods. The accumulation rates were 6.4, 9.8 and 8.4 cm/y, from 1959~2003,

412 2003~2010 and 2010~2014, respectively. For the Hangzhou Bay-QE system, the

413   accumulation rates in the three periods were 2.9, 4.2 and 3.8 cm/y, respectively. It is

414   obvious that, although the sediment load from the Changjiang River drastically

415   decreased in recent years, the deposition rate in the system did not decrease but actually

416   increased to a certain extent.

417

418   **4.4 Feedback of morphological evolution on hydrodynamics**

419   Hydrodynamics, sediment transport and bed evolution generally interact in nonlinear

420   fashion (e.g. Dronkers, 1986; Hibma et al., 2003; Yu et al., 2012; Winterwerp and

421   Wang, 2013). The asymmetry of the tide is one of the controlling factors for residual

422   sediment transport and hence morphological evolution of estuaries and tidal basins (e.g.

423   Aubrey, 1986; Dronkers, 1986; Friedrichs and Aubrey, 1988; Wang et al., 2002). In

424   estuaries, the tide is flood-dominant if the flood duration is shorter than the ebb

425   duration, and ebb-dominant if the opposite is true (Wang et al., 2002).

426

427   Figure 10a and 8b illustrates the time series of annually averaged high- and low-tide

428   levels and the tidal ranges, respectively, at the Ganpu gauging station. Since the 1970s,

429   the high-tide level has increased gradually from around 4.7 m to 5.4 m, whereas the

430   low-tide level remained stable around -2.6 m up to 2000 before increasing gradually to -

431   2.4 m since then. In accordance, the annually-averaged tidal range increased by about

432   0.6 m since the 1970s. The increasing high-tide level is caused by the land boundary

433   changes due to the coastal embankment which enhanced the tidal wave reflection (Xie

434   et al., 2005). A good relationship exists between the embanked area and the annual high

435   level (Fig. 11). An addition factor for the high tidal level increase is the increasing

436   occurrence of storm surges in the Hangzhou Bay area (Liu et al., 2016). The change in

437   the low-tide level was mainly related to the changes in bed level (Han et al., 2003).

438

439   Figure 10c illustrates the annually-averaged flood and ebb durations based on the water

440   level data at the Ganpu station. As can be seen, the duration of the flood is shorter than

441   that of the ebb. Before 1980, the flood duration was around 5 h 30 min and the ebb

442   duration around 6 h 50 min, the ratio between the two being constant around 0.85. Since

443   1981, the duration of the flood became gradually shorter, whereas that of the ebb

444   became gradually longer. From 1981 to 2015, the change in duration of both flood and

445   ebb was about 40 minutes. Subsequently, the ratio between the two gradually decreased

446   to 0.63. This reveals that the flood dominance of the inner Hangzhou Bay became

447   enhanced due to coastal embankment and sediment accumulation.

448

449   Figure 12 illustrates the relationships between the water and sediment fluxes across the

450   Jinshan transect and the tidal range at the Luchaogang gauging station at the time of the

451   cruises in 1983 and 2015. As can be seen, both water and sediment fluxes correlate well

452   with the tidal range. At a mean tidal range of 3.2 m, the water fluxes in 1983 and 2015

453   were 108×10^8 m^3 and 80×10^8 m^3, respectively, indicating that the gross water flux

454   decreased by about 25% over the last 30 years (Fig. 12a). The decrease in the tidal

455   prism is related to the decreasing tidal flat (e.g. Van der Wal et al., 2002; Winterwerp

456   and Wang, 2013). However, the sediment fluxes remained similar over the same period.

457   At the mean tidal range of 3.2 m, the sediment flux in the two reference years was

458   1.45×10^6 t.
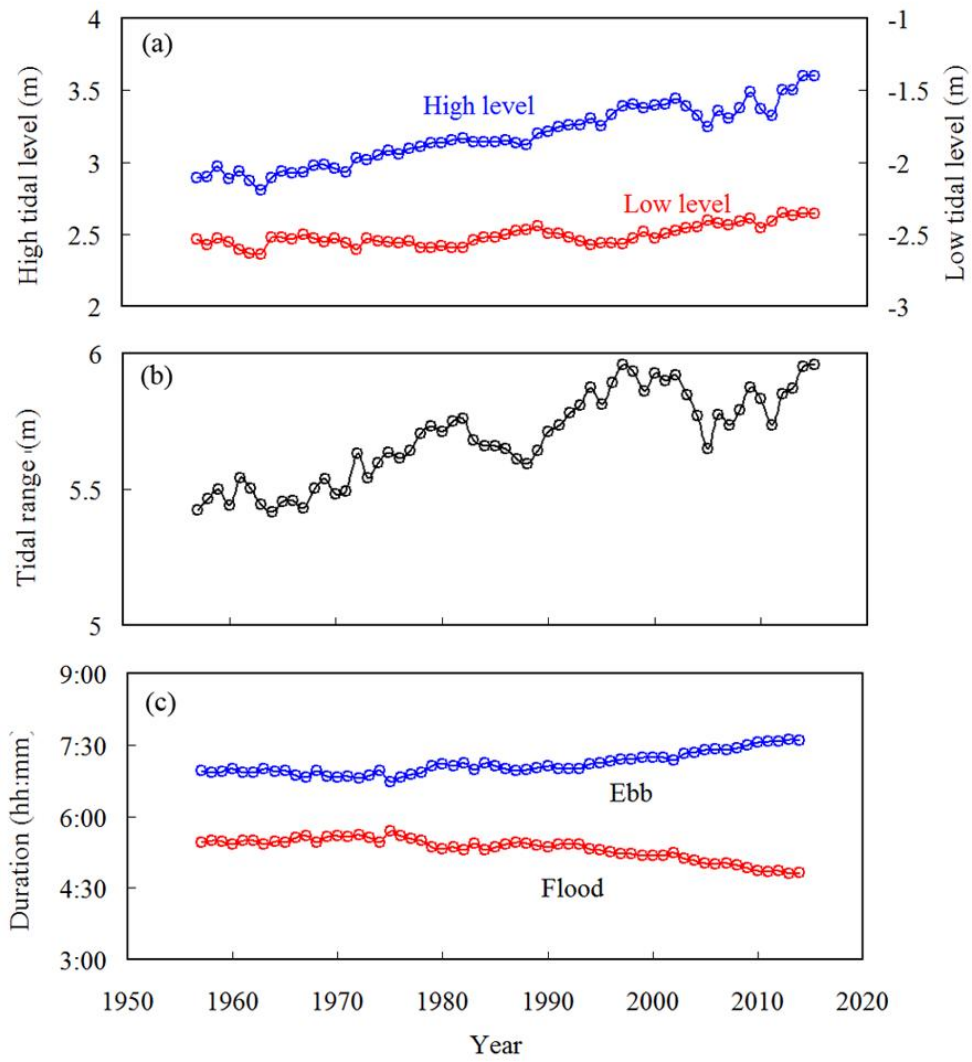
459

460   Fig. 10. Annually-averaged high- and low-tide levels (a), tidal range (b) and flood/ebb

461   durations at the Ganpu gauging station. (data from Zhejiang Hydrographic Office).
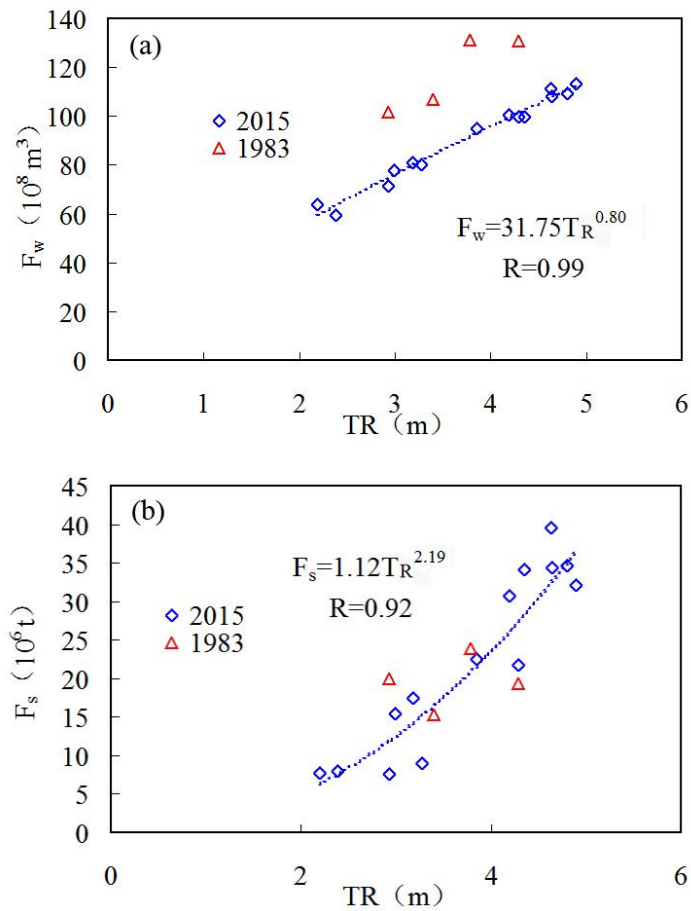
462
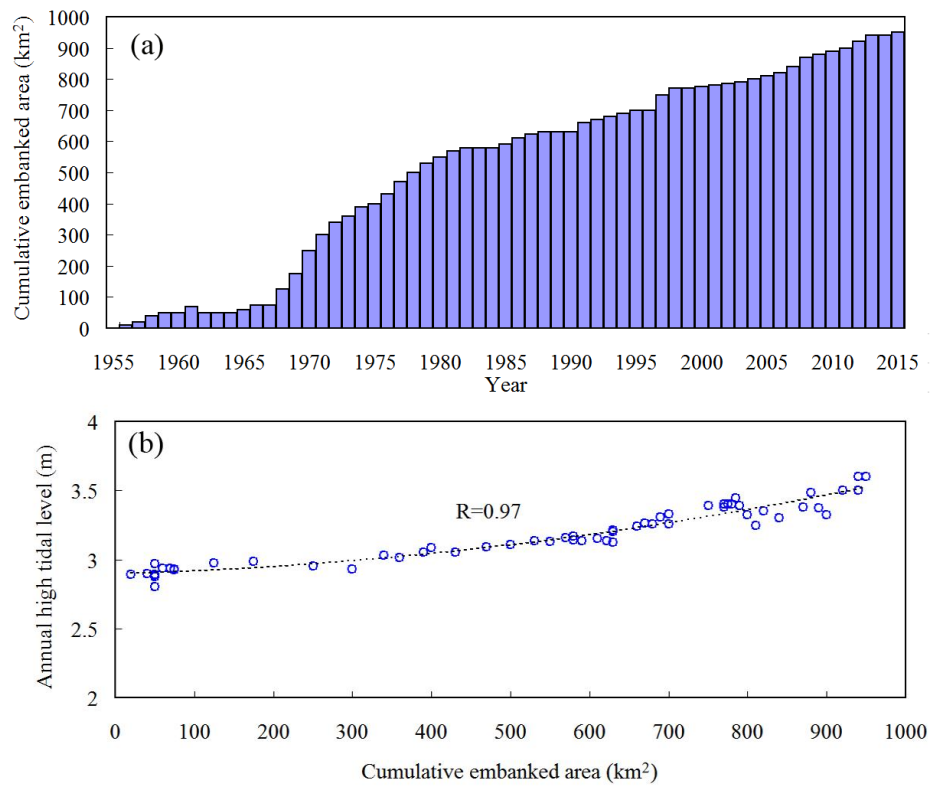
463

464 Fig. 11. Time series of the cumulative embanked area in the Qiantang – Hangzhou Bay

465 area (a) and the relationship between the cumulative embanked area and the annual high

466 tidal level at Ganpu station (b). Data in panel (a) is from Tang and Cao (2016).

467

Fig. 12. The relationships between flood/ebb-averaged water fluxes (F_w) (a) and sediment fluxes (F_s) (b) across the Jinshan transect versus the tidal range at the Luchaogang station (T_R) during the winter cruises of 1983 and 2015.

Because sediment flux is a function of water flux and suspended sediment concentration, it is obvious that the SSC increased in recent years. This is related to the stronger tidal currents caused by the narrowed cross-section. However, in comparison to the water fluxes, the net sediment flux is very small, being the difference between the very large flood and ebb fluxes, and is therefore extremely difficult to measure or compute with any degree of confidence (Townend, 2005). Given that the sediment flux has not changed, but that the flood dominance has been enhanced over the last 30 years,

480　it is reasonable to assume that, at present, more sediment is transported landward in one

481　tidal cycle. This explains the increasing accumulation rate in the inner Hangzhou Bay.

482

483　**5. Discussion**

484　**5.1 Influence of the decreasing sediment load from the Changjiang River**

485　The sediments in the Hangzhou Bay and the Qiantang Estuary are mainly derived from

486　the Changjiang River (e.g. Su and Wang, 1989; Chen et al., 1990). After the river-borne

487　sediments enter the Changjiang Estuary, about one-half is deposited within the estuary,

488　most of the other half being dispersed to the south, the remainder northward to the

489　Jiangsu coastal sea (Chen et al., 1985; Milliman et al., 1985). The reduction of the

490　Changjiang sediment load caused wide concern of what influence this would have on

491　sediment delivery to the Hangzhou Bay and the associated morphological development.

492

493　The results of the present analysis show that, in recent years, the sedimentation rates in

494　the Hangzhou Bay and the QE as a whole has not decreased, but rather increased to

495　some extent, as shown in Fig.7 and Table 2. This can be attributed to the adjustment of

496　the area of the outer Changjiang Estuary. The reduction of the sediment load from the

497　Changjiang River is mainly related to the flood season from June to September (e.g. Dai

498　et al., 2016; Xie et al., 2017). Recent research showed that in the outer Changjiang

499　estuary, the SSC has not decreased in the flood seasons of the last few decades (Xie et

500　al., 2017). During the last 7000 years of the post-glacial transgression, the large

501　amounts of sediment from the Changjiang formed an elongated, up to 50 m thick mud

502　belt that stretches from the Changjiang Estuary almost up to Taiwan (Liu et al., 2007).

503　The tides in this region play an important role in sediment transport. Large tidal ranges

504 and strong tidal currents, in combination with shallow water depths, small seabed slopes

505 and little wave action, have resulted in active resuspension of fine-grained sediment

506 from the local seabed (Gao et al., 2015).

507

508 As pointed out by Kennedy (1984), estuaries trap significant quantities of material and

509 thus act as filters between land and the oceans. The principal sediment supply of the

510 Hangzhou Bay is neither from the Qiantang River nor directly from the Changjiang

511 River. Instead, there are two filters, i.e. the Changjiang Estuary and the mud area in the

512 outer Changjiang Estuary. The drastic reduction in the sediment load of the Changjiang

513 River would thus initially be recorded in two buffer areas. This can be supported by the

514 recent study of Yang et al (2011) and Luo et al (2017) who found that the Changjiang

515 subaqueous delta is experiencing overall net erosion since the construction of the Three

516 Gorges Dam in 2003 and suggested that the delta recession will continue to occur in the

517 near future because the Changjiang sediment discharge will further decrease in the near

518 future due to the construction of new dams. On the other hand, recent hydrological

519 surveys revealed that the annually-averaged net sediment flux into the Hangzhou Bay

520 has decreased slightly by about 10% after 2003 (Xie et al., 2017), whereas the net

521 sediment fluxes in the coastal area south of Zhoushan islands have not detected to be

522 decreased apparently in last decades (Deng et al., 2017). The slight decrease sediment

523 supply at the mouth of the bay caused the erosion in the outer bay in recent years (Fig.

524 7b and c). Its influence on the inner bay and the QE has been overcome by the coastal

525 embankment, because the sediment in the inner bay and the QE comes from the outer

526 bay (Chen et al., 1990). This phenomenon agrees with the long-term morphodynamic

527 model by Yu et al (2012) that with the sediment supply decrease at the seaside of the

528 estuary, erosion will firstly observed at the mouth area. The morphological effects on

529 the inner bay and the QE are expected to lag behind by a relatively longer time.

530

5.2 Morphological development of the southern flat

532 Tidal flats are important geomorphological units in estuarine and coastal environments,

533 which provide habitat for wild lifes, resources for land reclamation and protection

534 against extreme storm events, and play an important role in global carbon cycling and

535 climate change (e.g. Allen and Pye, 1992; Yang et al., 2005; De Vriend et al., 2011;

536 Friedrichs, 2011). The accreting southern tidal flat in the Hangzhou Bay plays as a sink

537 for sediment from Changjiang Estuary under the role of the secondary plume of

538 Changjiang Estuary, also for the sediment output from the QE during high river flow

539 season or years (Li and Xie, 1993). In the last centuries, the flat advanced fast with the

540 average rate of about 25 m/y and vertical sedimentation rate of about 5 cm/y, under

541 natural condition (Chen et al., 1990).

542

543 The strong sedimentation of the southern flat is related to the large-scale flow patterns

544 in the Hangzhou Bay. The northern bay is dominated by flood currents while the

545 southern bay is dominated by ebb currents (e.g. Cao et al., 1985; Su and Wang, 1989;

546 Xie et al., 2009). Ebb currents diverge at the front of the southern flat due to the

547 increasing cross-sectional width. Subsequently, the sediment transport capacity of ebb

548 currents decreased, and strong sedimentations occur (Cao et al., 1985; Han et al., 2003).

549 Because the embankments in the last decades have been mainly carried out above MSL,

550 the changes of large-scale flow patterns has been limited (Shao, 2016). In addition,

551 SSCs in the front of tidal flat area is high, with the vertically averaged SSC usually

552   above 3 kg/m^3 (Fig. 5). The sedimentation rate of the southern flat has been increased

553   apparently in the last decades, compared to the above-mentioned rate of about 5 cm/y in

554   natural conditions (Fig. 8). This is probably related to the increasing SSC in the front

555   area. Recent study of Van Maren et al (2016) revealed that land reclamations in

556   estuaries will lead to an increase in SSC because of the decrease in accommodation

557   space for fine-gained sediments. This can also be evaluated from the fact that despite

558   the water fluxes into the inner bay have decreased apparently since 1980s, the sediment

559   fluxes can be more or less maintained (Fig. 12).

560

561   The cross-sectional profiles of the accretion-dominated tidal flat are normally convex

562   (Fig. 8), similar to other accretional intertidal flats in the world (Kirby, 2000; Yang et

563   al., 2005; Friedrichs, 2011; Wang et al., 2014). Apparent reductions in width of the

564   southern flat, due to coastal embankments by building sea dykes, have resulted in

565   steeper fronts. This is similar to the observations in the Changjiang Estuary and Jiangsu

566   coast (Yang et al., 2005; Van Maren et al., 2013; Wang et al., 2014). Wind waves can

567   cause erosion on the wide intertidal flat (Kirby, 2000; Yang et al., 2005; Wang et al.,

568   2014). The reduction in the intertidal flat width can cause a concentration of wave

569   energy on the lower flat and in the sub-tidal area, with relative deep water, resulting in

570   bed erosion (Wang et al., 2014). A model applied to the accreting intertidal flat shows

571   that tidal flats with abundant sediment supply can persistently prograde with the similar

572   slope, remaining in the equilibrium shape under natural conditions (Liu et al., 2010).

573   However, southern flat in the Hangzhou Bay is not the case. The font area of the flat has

574   become progressively steeper because of the constraint by the main channel of the bay.

575

576   **5.3 Morphological response model of the Hangzhou Bay**

577 Over the last decades, the annual tidal levels in the outer Changjiang Estuary and in the

578 Hangzhou Bay have fluctuated around their multi-year averages. Hence the influence of

579 sea-level rise on sediment transport and morphological evolution of the Hangzhou Bay

580 have been minor. The main channel of the QE used to meander continuously, and the

581 coastal wall revetments used to collapse frequently, resulting in serious economic losses

582 and even losses of human lives, besides making the development of resources such as

583 navigation channel maintenance difficult. Since the 1960s, large-scale coastal

584 embankments in the QE have been carried out for the purpose of flood defense, urban

585 land requirements, etc. (Li and Dai, 1986; Han et al., 2003; Pan et al., 2010).

586 Embankments occurred gradually over time (Fig. 3a and 7), having to date resulted in

587 more than 1000 km^2 of reclaimed tidal flats. In the process, the estuarine width was

588 greatly reduced, for example from about 10 km to 2.5 km at Yanguan and from about

589 22 km to18 km at Ganpu.

590

591 The morphological response in the QE is related to progressive coastal embankment.

592 Before 2006, the QE and the inner Hangzhou Bay showed sediment accretion (Fig. 9).

593 The accumulation in the QE needed sediment supply from downstream (i.e. the inner

594 Hangzhou Bay). After 2006, when the morphological evolution in the QE has been

595 basically stable, accumulation shifted downstream. As a consequence, the accumulation

596 rate in the inner Hangzhou Bay increased (Fig. 7 and 9), the sediment source being the

597 outer Hangzhou Bay. This is consistent with Chen et al (1990), who showed, based on

598 sedimentological analysis, that the sediment in the QE comes mainly from the

599 Hangzhou Bay, whereas the sediment in the inner Hangzhou Bay derives mainly from

600 the outer bay. Overall, the sediment accretion in the Hangzhou Bay and the QE is

601 characterized by the gradually seaward shifting trend.

602

603 Worldwide, land reclamation and dredging have been, and still are, common practice in

604 many estuaries, many researchers reporting increased sedimentation as a consequence

605 (e.g. Inglish and Kestner, 1958; Sherwood et al., 1990; Pye and French, 1993; Van der

606 Wal et al., 2002). This can mainly be attributed to enhancement of flood dominance due

607 to decrease tidal flat area (Van der Spek, 1997). In the viewpoint of the estuarine

608 convergence, stronger convergence results in the large longitudinal sandbar in the QE

609 shifts seaward (Yu et al., 2012). The increasing sedimentations in the Hangzhou Bay-

610 QE system in last decades observed in this study agree with their numerical model

611 results.

612

613 In response, the northern bay-mouth switched from a depositional mode to an erosional

614 mode in recent years. This is in agreement with previous observation by Dai et al

615 (2014). Besides the above-mentioned causes, there are probably several other factors.

616 First, there are probably direct sediment exchanges between the northern bay mouth and

617 southern CE mouth across the front of the Nanhui shoal (Su and Wang, 1989; Chen et

618 al., 1990). With the reduction of the Changjiang sediment load, the progradation rates of

619 tidal flats along the CE slowed down or even reversed to erosion (Yang et al., 2005;

620 Van Maren et al., 2013; Wang et al., 2015). Hence the SSC in the outer CE has

621 decreased by about 20-30% after the Three Gorges Dam construction in 2003 (Li et al.,

622 2012; Xie et al., 2017). The SSC decrease of the outer CE would decrease the direct

623 sediment supply to the northern Hangzhou Bay. On the other hand, more than 150 km^2

624 along the Nanhui shore of the northern mouth has been reclaimed since the 1980s (Fig.

625 3b). The reclamation intercepted large amounts of sediment, which could be originally

626 transported into the northern Hangzhou Bay. On the other hand, the eastward

627 propagation of the Nanhui flat by about 10 km in recent years has increased the distance

628 and changed the route by which Changjiang sediment can enter the Hangzhou Bay (Fig.

629 3b).

630

631 **5.4 Future morphological evolution trends**

632 Progressive land reclamation in coastal environments continually change the

633 circumjacent hydrodynamics and sediment transport (e.g. Van der Spek, 1997; Van der

634 Wal., et al., 2002; Wang et al., 2015). During the last decades, both the annually-

635 averaged high and low tidal levels in the inner bay have been increased due to shoreline

636 constriction and sediment accumulation. The annually-averaged durations of rising and

637 falling tides have been shorten and lengthened, respectively, indicating that the flood

638 dominance in the inner bay has been enhanced (Fig. 10). As a result, the net landward

639 sediment flux over one tidal cycle at the interface between the inner and outer bay has

640 been increased to some extent (Fig. 12). In return, this nonlinear feedback mechanism

641 has promoted the sediment accumulation in the inner bay.

642

643 At present, the large-scale coastal embankments in the QE have continuously increased

644 the constriction of the estuary over several decades. In the near future, only some local

645 areas will be reclaimed (Pan et al., 2010). However, the sediment accumulation will not

646 cease synchronously due to the enhanced flood-dominance and landward sediment

647 transport. The temporal scales of estuarine morphodynamics are related to the spatial

648   scales involved (De Vriend, 1996). The larger the spatial scale is, the longer the time

649   that would be needed for the morphological adjustment. In view of the large spatial

650   scale of the Hangzhou Bay and the complex sediment transport behavior, the timescale

651   for morphological readjustment in the Hangzhou Bay is expected to be in the order of

652   several decades. The accumulation trend of the inner bay will continue for some time,

653   while erosion of the outer bay will also continue in order to supply sediment to the inner

654   part.

655

656   **6. Conclusions**

657   Although the sediment load from the Changjiang River has reduced, especially since

658   2003 when the Three Gorges Dam was constructed and operated, the sedimentation rate

659   in the adjacent Hangzhou Bay has not decreased as expected. The outer Changjiang

660   Estuary acts as a buffer area and sediment sources for the Hangzhou Bay. Besides other

661   reasons, such as land reclamation in the Qiantang and Changjiang estuaries, the

662   documented erosion in the northern Hangzhou Bay can be partly attributed to the drastic

663   reduction of the Changjiang sediment load because that part directly exchanges

664   sediment with the Changjiang Estuary.

665

666   The large-scale human interventions played an important role in the morphological

667   evolution of the Hangzhou Bay-Qiantang Estuary system. The coastal embankment

668   increased the estuarine constriction and, to a certain extent, enhanced the flood

669   dominance in the inner part. Subsequently, the sedimentation rate in the estuary

670   increased. The morphological changes have been related mainly to the implementation

671   process of the coastal embankment. With progressive seaward coastal embankment,

672   sediment accumulation has resulted in gradual seaward aggradation. The annually-

673   averaged high and low tidal levels in the inner bay have been increased and the flood

674   dominance in the inner bay has been enhanced apparently. The tidal prism at the

675   interface between the inner and outer bay has decreased by about 25% since 1980s,

676   while the net landward sediment flux has been intensified to a certain extent. The

677   enhancing flood dominance and landward sediment transport are responsible for the

678   increasing sedimentation in the estuary. Furthermore, stronger sedimentations have

679   occurred at the southern shoreline, and the upper and sub-tidal flat has been steeper due

680   to coastal embankments and the constraint of the main channel of the bay. Although the

681   coastal embankment will cease in the near future, the morphological response is

682   expected to continue on for a longer time.

683

690
691   References

692   Allen, J.R.L., Pye, K., 1992. Coastal saltmarshes: their nature and importance. In: Allen,

693   J.R.L., Pye, K. (Eds.), Saltmarshes, Morphodynamics, Conservation and Engineering

694   Significance. Cambridge Uni. Press, Cambridge, U.K, pp. 1-18.

695   Aubrey, D.G., 1986. Hydrodynamic controls on sediment transport in well-mixed bays

696   and estuaries. In: Van de Kreeke, J. (Ed.), Physics of Shallow Estuaries and Bays.

697   Lecture Notes on Coastal and Estuarine Studies Vol. 16. Springer-Verlag, Berlin, pp.

698   245–276.

699   Blott, S.J., Pye, K., Van der Wal, D., Neal, A., 2006. Long-term morphological change

700   and its causes in the Mersey Estuary, NW England. Geomorphology 81(1-2), 185–206.

701   Burrough, P.A. McDonnell, R.A., 1998. Principles of Geographical Information

702   Systems. Oxford University Press, Oxford, UK, 352 pp.

703   Cao, P.K., Gu, G.C., Dong, Y.F., Hu, F.X., 1985. Basic characteristics of sediment

704   transport in Hangzhou Bay. J. East China Normal Uni., (3), 75-84 (in Chinese with

705   English abstract).

706   Chen, J.Y., Wang, B.C., Yu, Z.Y., 1989. Developments and Evolution of China's Coast.

707   Shanghai Sci. Tech. Pub., Shanghai, 556 pp (in Chinese).

708   Chen, J.Y., Zhu, H.F., Dong, Y.F., Sun J.M., 1985. Development of the Changjiang

709   Estuary and its submerged delta, Cont. Shelf Res. 4, 47-56.

710   Chien, N., Sie, H. S., Chow, C. T., Lee, Q.P., 1964. The fluvial processes of the big

711   sand bar inside the Chien Tang Chiang Estuary. Acta Geograph. Sin., 30(2), 124-142 (in

712   Chinese with English abstract).

713   Dai, Z.J., Fagherazzi, S., Mei, X.F., Gao, J.J., 2016. Decline in suspended sediment

714   concentration delivered by the Changjiang (Yangtze) River into the East China Sea

715   between 1956 and 2013. Geomorphology 268, 123–132.

716   Dai, Z.J., Liu, J.T., Xie, H.L. Shi W.Y., 2014. Sedimentation in the Outer Hangzhou

717   Bay, China: the influence of Changjiang sediment load. J. Coast. Res. 30, 1218–1225.

718   Deng, B., Wu, H., Yang, S.L., Zhang, J., 2017. Longshore suspended sediment transport

719   and its implications for submarine erosion off the Yangtze River Estuary. Estuarine

720   Coastal Shelf Sci. 190, 1-10.

721   De Vriend, H.J., 1996. Mathematical modelling of meso-tidal barrier island coasts. Part

722   I: Emperical and semi-emperical models, In: Liu, P.L.F. (Ed.), Advances in Coastal

723   Ocean Engineering. World Scientific, Singapore, pp. 115-149.

724   De Vriend, H.J., Wang, Z.B., Ysebaert, T., Herman, P.M.J., Ding, P.X., 2011. Eco-

725   Morphological Problems in the Yangtze Estuary and the Western Scheldt. Wetlands,

726   31(6), 1033-1042.

727   Dronkers, J., 1986. Tidal asymmetry and estuarine morphology. Nether. J. Sea. Res. 20

728   (2/3), 117–131.

729   Dyer, K.R., 1997. Estuaries - physical introduction, 2nd ed. John Wiley and Sons,

730   Chichester. 195 pp.

731 Editorial Committee for Chinese Harbors and Embayment (ECCHE), 1992. Chinese
732 Harbors and Embayment (Part V).. China Ocean Press, Beijing. 357pp (in Chinese).

733 Eisma, D., 1998. Intertidal deposits: river mouth, tidal flats, and coastal lagoons. CRC
734 Press, Boca Raton. 495pp.

735 Fan, D.D., Tu, J.B., Shang, S., Cai, G.F., 2014. Characteristics of tidal-bore deposits
736 and facies associations in the Qiantang Estuary, China. Mar. Geol. 348, 1-14.

737 Fairbridge, R.W., 1980. The estuary: its definition and geodynamic cycle. In: Olausson,
738 E., Cato, I. (Eds.), Chemistry and Biogeochemistry of Estuaries. John Wiley & Sons,
739 New York, NY, pp. 1-36.

740 Friedrichs, C.T., 2011. Tidal flat morphodynamics: a synthesis. In: Hansom, J.D. and
741 Flemming, B.W. (eds), Treatise on estuarine and coastal science, vo.3: Estuarine and
742 coastal geology and geomorphology. Elsevier, pp. 34.

743 Friedrichs, C.T., Aubrey, D.G., 1988. Non-linear tidal distortion in shallow well-mixed
744 estuaries: a synthesis. Estu. Coast Shelf Sci. 27, 521-45.

745 Gao, S., Wang, Y.P., 2008. Material fluxes from the Changjiang River and their
746 implications on the adjoining continental shelf ecosystem. Cont. Shelf Res. 28, 1490-
747 1500.

748 Gao, S., Wang, D.D., Yang, Y., Zhou, L., Zhao, Y.Y., GAO, W.H., Han, Z. C., YU, Q.,
749 Han, Z.C., Dai, Z.H., Li, G.B., 2003. Regulation and Exploitation of Qiantang Estuary.
750 China Water Power Press, Beijing, 554pp (in Chinese).

751 Hibma, A., Stive, M.J.F., Wang, Z.B., 2004. Estuarine morphodynamics. Coast. Eng.
752 51, 765-778.

753 Inglish, C.C., Kestner, F.J.T., 1958. The long-term effects of training walls,
754 reclamation, and dredging on estuaries. Proc. Institution Civil Eng. 9, 193–216.

755 Kirby, R., 2000. Practical implications of tidal flat shape. Cont. Shelf Res. 20, 1061-
756 1077.

757 Kennedy, V. S., 1984. The estuary as a filter. Academic Press, New York. 511pp.

758 Lane, A., 2004. Bathymetric evolution of the Mersey Estuary, UK, 1906-1997: causes
759 and effects. Estu. Coast. Shelf Sci. 59, 249–263.

760 Li, G.B., Dai, Z.H., 1986. Fluvial processes and reclamation of the Qiantang Estuary.
761 Inter. J. Sed. Res. 1(1), 56–66.

762 Li, P., Yang, S.L., Milliman, J.D., Xu, K.H., Qin, W.H., Wu, C.S. , Chen, Y.P. , Shi,
763 B.W., 2012. Spatial, temporal, and human-induced variations in suspended sediment
764 concentration in the surface waters of the Yangtze Estuary and adjacent coastal areas.
765 Estu. Coast. 35, 1316–1327.

766 Li, Y., Xie, Q.C., 1993. Dynamical development of the Andong tidal flat in Hangzhou
767 Bay, China. Donghai Mar. Sci. 11(2), 25-33 (in Chinese with English abstract).

768 Liu, J.P., Xu, K.H., Li, A.C., Milliman, J.D., Velozzi, D.M., Xiao, S.B., Yang, Z.S.,
769 2007. Flux and fate of Yangtze River sediment delivered to the East China Sea.
770 Geomorphology 85(3-4), 208–224.

771 Liu, X.J., Gao, S., Wang, Y.P., 2011. Modeling profile shape evolution for accreting
772 tidal flats composed of mud and sand: A case study of the central Jiangsu coast, China.
773 Cont. Shelf Res. 31(16): 1750-1760

774 Liu, Y.F., Xia, X.M., Chen, S.L., Cai, T.L., 2016. Morphological evolution of Jinshan
775 Trough in Hangzhou Bay (China) from 1960 to 2011, Estuar. Coast. Shelf Sci. In press.

776 Luo, X.X., Yang, S.L., Wang, R.S., Zhang, C.Y., Li, P., 2017. New evidence of
777 Yangtze delta recession after closing of the Three Gorges Dam. Sci. Rep. 7, 41735.

778 Milliman, J.D., 1997. Blessed dams or damned dams, Nature 386, 325–326.

779 Milliman, J.D., Farnsworth, K.L., 2011. River discharge to the coastal ocean—A global
780 synthesis. Cambridge Uni. Press, Cambridge, UK. 394pp.

781 Milliman, J.D., Shen, H.T., Yang, Z.S., Robert, H.M., 1985. Transport and deposited of
782 river sediment in the Changjiang estuary and adjacent continental shelf. Cont. Shelf
783 Res. 4, 37-45.

784 Pan, C.H., Shi, Y.B., Han, Z.C., 2010. Regulation of Qiantang River estuary and
785 scientific and technological innovations. China Water Resour. 14, 13–16 (in Chinese
786 with English abstract).

787 Pye, K., French, P.W., 1993. Erosion and accretion processes on British Saltmarshes,
788 Vol. 5. Cambridge Environ. Res. Cons., Cambridge.

789 Shao, M.M., 2016. Impacts of reclamation of tidal dynamics in Hangzhou Bay. M.Sc.
790 thesis, Zhejiang University.

791 Sherwood, C.R., Jay, D.A., Harvey, R.B., Hamilton, P., Simenstad, C.A., 1990.
792 Historical changes in the Columbia river estuary. Prog. Oceanogr. 25, 299–352.

793   Su, J.L., Wang, K.S., 1989. Changjiang River plume and suspended sediment transport
794   in Hangzhou Bay. Cont. Shelf Res. 9(1), 93–111.

795   Syvitski, J.P.M., Vörösmarty, C.J., Kettner, A.J., Green, P., 2005. Impact of humans on
796   the flux of terrestrial sediment to the global coastal ocean. Science 308(15), 376–380.

797   Tang, Z.W., Cao, Y., 2016. Beach resources evolution and trend analysis of Qiantang
798   River estuary section under the condition of Narrowing river. Zhejiang Hydrotec., (2):
799   20-23.

800   Townend, I., 2005. An examination of empirical stability relationships for UK estuaries.
801   J. Coast. Res. 21, 1042–1053.

802   Townend, I., Whitehead, P., 2003. A preliminary net sediment budget for the Humber
803   Estuary. Sci. Total Environ. 314–316, 755–767.

804   Trenhaile, A.S., 1997. Coastal Dynamics and Landforms. Clarendon, Oxford, UK.
805   382pp.

806   Van der Spek, A.J.F., 1997. Tidal asymmetry and long-term evolution of Holocene tidal
807   basins in The Netherlands: simulation of palaeo-tides in the Schelde estuary. Mar. Geol.
808   141, 71–90.

809   Van der Wal, D., Pye, K., Neal, A., 2002. Long-term morphological change in the
810   Ribble Estuary, northwest England. Mar. Geol. 189, 249–266.

811   Van der Wal, D., Pye, K., 2002. The use of historical bathymetric charts to assess
812   morphological and sediment budget change in estuaries. Geogr. J. 169(1), 21–31.

813   Van Maren, D.S., Yang, S.L., He, Q., 2013. The impact of silt trapping in large
814   reservoirs on downstream morphology: the Yangtze River. Ocean Dyn. 63, 691–707.

815   Van Maren, D.S., Oost, A.P., Wang, Z.B., Vos, P.C., 2016. The effect of land
816   reclamations and sediment extraction on the suspended sediment concentration in the
817   Ems Estuary. Mar. Geol. 376, 147-157.

818   Wang, Y.P., Gao, S., Jia J.J., Thompson, C.E.L., Gao, J.H., Yang, Y., 2012. Sediment
819   transport over an accretional intertidal flat with influences of reclamation,Jiangsu coast,
820   China. Mar. Geol. 291-294, 147-161.

821   Wang, Z.B., Jeuken, M.C.J.L., Gerritsen, H., De Vriend, H.J., Kornman, B.A., 2002.
822   Morphology and asymmetry of the vertical tide in the Wester-Schelde estuary. Cont.
823   Shelf. Res. 22, 2599–2609.

824 Wang, Z.B., Van Maren, D.S., Ding, P.X., Yang, S.L., Van Prooijen, B.C., De Vet,
825 P.L.M., Winterwerp, J.C., De Vriend, H.J., Stive, M.J.F., He, Q., 2015. Human impacts
826 on morphodynamic thresholds in estuarine systems. Cont. Shelf Res. 111, 174–183.

827 Whitehouse, R.J.S., 2002. Predicting estuary morphology and process: an assessment of
828 tools used to support estuary management. In: Editor (ED.), Proc. Seventh Inter. Conf.
829 on Estu. Coast. Model., St. Petersburg, Florida, USA, 2001, pp. 344–363.

830 Winterwerp, J.C., Wang, Z.B., 2013. Man-induced regime shifts in small estuaries – I:
831 theory. Ocean Dyn. 63(11), 1279–1292.

832 Xie, D.F., Pan, C.H., Wu, X.G., Gao, S., Wang, Z.B., 2017. The variations of sediment
833 transport patterns in the outer Changjiang Estuary and Hangzhou Bay over the last 30
834 years. J. Geophy. Res. Ocean, 122, doi:10.1002/2016JC012264.

835 Xie, D.F., Gao, S., Wang, Z.B., De Vriend, H.J., 2009. Numerical modeling of tidal
836 currents, sediment transport and morphological evolution in Hangzhou Bay, China.
837 Cont. Shelf. Res. 28, 316–328.

838 Xue, H.C., 1995. Deposition character of Changjiang estuary in the past 100 years. In:
839 Editor (Ed.), Proc. 17th Symposium on Coastal Engineering. Publisher, Beijing (in
840 Chinese).

841 Xie, Y.L., Huang, S.C., Wang, R.F., Zhao, X., 2005. Numerical simulation of effects of
842 reclamation in Qiantang Estuary on storm surge at Hangzhou Bay. Ocean Eng. 25(3),
843 61-67 (in Chinese with English abstract).

844 Yang, S.L., Zhang, J., Zhu, J., Smith, J.P., Dai, S.B., Gao, A., Li, P., 2005. Impact of
845 dams on Yangtze River sediment supply to the sea and delta intertidal wetland response.
846 J. Geophy. Res. 110, F03006.

847 Yang, S.L., Milliman, J.D., Li, P., Xu, K., 2011. 50, 000 dams later: erosion of the
848 Yangtze River and its delta. Glob. Planet. Change 75(1-2), 14–20.

849 Yu, J., Cao, Y., 2006. Sediment deposition after regulation and reclaiming of Qiantang
850 Estuary. J. Sed. Res. (1), 17–24 (in Chinese with English abstract).

851 Yu, Q., Wang, Y., Gao, S., Flemming, B., 2012. Modeling the formation of a sand bar
852 within a large funnel-shaped, tide-dominated estuary: Qiantangjiang Estuary, China.
853 Mar. Geol. 299–302, 63–76.

854

Table 1. Accumulation and erosion in Hangzhou Bay in different periods.

Time interval	Volume changes (10^6 m^3)				Accumulation rate (cm/y)			
	Zone A	Zone B	Zone C	Hangzhou Bay	Zone A	Zone B	Zone C	Hangzhou Bay
1887~1937				1800				0.8 a
1937-1987				3700				1.5 a
1959~2003	1715	724	2729	5168	2.4	1.0	3.9	2.4
2003~2010	952	-466	606	1092	9.0	-4.0	5.8	3.3
2010~2014	771	-126	-75	571	13.4	-1.9	-1.3	3.0

*Positive values denote sediment accumulation while negative values denote sediment erosion. The same below.

[a] Based on the data from Xue (1995).

Table 2. Net accumulation in the Hangzhou Bay-Qiantang Estuary system in different time intervals.

Time intervals	Hangzhou Bay		Qiantang Estuary		Hangzhou Bay-Qiantang Estuary system	
	VC	AR	VC	AR	VC	AR
1959~2003	5168	2.4	1916	6.4	7084	2.9
2003~2010	1092	3.3	477	9.8	1569	4.2
2010~2014	571	3.1	231	8.4	802	3.8

*VC: volume changes, in 10^6 m^3; AR: accumulation rate, in cm/y.

864   **Figure Captions**

865   Fig. 1. Temporal variations of annual water and sediment discharges measured at the

866   Datong gauging station located at the tidal limit 640 km upstream from the Changjiang

867   River mouth (data from the Changjiang River Hydraulic Engineering Committee).

868   Fig. 2. Locations in Hangzhou Bay referred to in the text. The dashed lines depict water

869   depths. The definitions of the three zones referred to in the statistics of Tables 1 are also

870   given.

871   Fig. 3. Coastal embankment in the Qiantang Estuary (a) and land reclamations in front

872   of the Nanhui flat bordering the Changjiang Estuary (b).

873   Fig. 4. Surface sediment grain size in Hangzhou Bay (from Xie et al., 2009).

874   Fig. 5. Suspended sediment concentration distribution during spring tide in the

875   Hangzhou Bay (modified from Han et al., 2003).

876   Fig. 6. The cross-sections illustrated in Fig. 8 and the hydrographic stations of 1983 (red

877   cycles) and 2015 (blue cycles).

878   Fig. 7. Rates of morphological change in Hangzhou Bay over successive periods: (a)

879   1959~2003; (b) 2003~2010; and (c) 2010~2014. The black areas denote land

880   reclamation and the shading areas denote the original shoreline and the latest

881   reclamation.

882   Fig. 8. Bed level changes along the cross-sections depicted in Fig. 6.

883   Fig. 9. Temporal changes in channel volumes below mean high-tide level in the

884   Qiantang Estuary and the inner Hangzhou Bay (zone A in Fig.2).

885   Fig. 10. Annually-averaged high- and low-tide levels (a), tidal range (b) and flood/ebb

886   durations at the Ganpu gauging station. (data from Zhejiang Hydrographic Office).

887   Fig. 11. Time series of the cumulative embanked area in the Qiantang – Hangzhou Bay

888   area (a) and the relationship between the cumulative embanked area and the annual high

889   tidal level at Ganpu station (b). Data in panel (a) is from Tang and Cao (2016).

890   Fig. 12. The relationships between flood/ebb-averaged water fluxes (F_w) (a) and

891   sediment fluxes (F_s) (b) across the Jinshan transect versus the tidal range at the

892   Luchaogang station (T_R) during the winter cruises of 1983 and 2015.

893